THE QUASILOCAL IMPURITY STATES IN THE THERMOELECTRIC Bi_2Te_3-BASED COMPOUNDS

M.K. Zhitinskaya[1], Yu.G. Ispolov[1], S. Nemov[1], A.A. Muhtarova[1], T.E. Svechnikova[2]
([1]State Polytechnical University, 29, Polytekhnicheskaya Str., St. Petersburg, 195251, Russia;
[2]Baikov Institute of Metallurgy, Russian Academy of Sciences,
49, Leninsky Ave., Moscow, 119991, Russia)

- *The thermoelectric figure of merit of homogeneous crystals is significantly higher than that of inhomogeneous crystals, all other factors being equal. We consider the possibility of getting highly homogeneous crystals by introducing a nonconventional doping impurity for A^5B^6 compounds, namely Sn impurity. Doping of Bi_2Te_3 crystals with tin is accompanied by formation of quasilocal impurity states on the background of the allowed energy spectrum that are located close to the top of valence band additional extremum. High density of these states results in the stabilization of chemical potential and the enhancement of the electrical homogeneity of crystals. In this paper, we study the influence of isovalent substitution of atoms in Bi- or Te-sublattices in Bi_2Te_3:Sn monocrystals. The Nernst-Ettingshausen constants Q_{ikl} and the basic kinetic coefficients: electrical conductivity σ_{ii}, the thermoelectric power S_{ii}, Hall coefficients R_{ikl} were measured. All the crystals were grown by the Czochralski technique. Depending on the composition, the samples were of n- or p-type conductivity. It was found that with a substitution of Sb atoms for Bi and Se atoms for Te, in Bi_2Te_3:Sn crystals there is retained formation of quasilocal tin states in the valence band. Besides, in all crystals with tin there was found a more homogeneous distribution of current carrier concentration. The thermoelectric figure of merit of n-type samples reached maximum value $Z = 3.3 \cdot 10^{-3}$ K^{-1} in the temperature range 340 – 370 K. It was supposed that the quasilocal states placed in the valence band interact with the basic electron states and produce a considerable effect on the properties of n-$Bi_2Te_{2.85}Se_{0.15}$.*

Introduction

Traditional application of Bi_2Te_3-based solid solutions in thermoelectric converters motivates a search for methods to improve their properties. To create materials with high thermoelectric properties, these materials are doped with various impurities. However, the addition of impurities usually leads to significant fluctuations of thermoelectric properties associated with the statistical character of the spatial impurity distribution.

According to [1-3] it was established that on introducing of *Sn* impurity into Bi_2Te_3, quasilocal states appear within the valence band near the top of the additional extremum. The quasilocal states lead to pinning of the Fermi level. Since the thermoelectric power is sensitive to variation of the Fermi level, the quasilocal states lead to its stabilization and the enhancement of homogeneity that was proved by investigations of the Seebeck coefficient distribution over the surface of crystals with scanning microprobe [3] and by *X*-ray diffraction microanalysis [4]. This is particularly important for crystals of the A^VB^{VI} trigonal system that exhibit a pronounced anisotropy. Under real growth conditions, even the best single crystals of this compound comprise many inhomogeneities. The thermoelectric figure of merit is known to be higher in homogeneous crystals. Hence, different possibilities may be considered to obtain a material with high homogeneity. One of them is to use the Czochralski technique [5]. Another way is to use doping impurities (*Sn*) creating quasilocal states in the compound. We used both of these approaches in our investigation.

We investigated the effect of *Sn* atoms addition on the thermoelectric properties of Bi_2Te_3 under substitution of the part of atoms in *Bi*- or *Te* sublattices.

1. Experiment

The Nernst-Ettingshausen constants Q_{ikl} and the basic kinetic coefficients: electrical conductivity σ_{ii}, the thermoelectric power S_{ii}, Hall coefficients R_{ikl} were measured on single crystals of *Sn*-doped Bi_2Te_3, $Bi_{1.99}Sb_{0.01}Te_3$ and $Bi_2Te_{3-x}Se_x$ ($x = 0.06$; 0.12) in the temperature range from 77 to 420 K. All single crystals were grown by the Czochralski technique with replenishment of the melt from a liquid phase [5]. The single crystals were grown in the [1010] direction normal to the main crystallographic axis *c*. The carrier density was determined from the expression $n, p = [q\, R_{321}(77\ \mathrm{K})]^{-1}$.

The spatial distribution of thermoelectric power over the surface of $Bi_2Te_{3-x}Se_x$:*Sn* single crystals was investigated by microprobe method described in [6].

2. Results

2.1. Influence of resonant states on free holes concentration

Doping Bi_2Te_3 crystals with tin is accompanied by the formation of a band of resonant states on the background of the allowed valence band spectrum. The resonant states lead to pinning of the Fermi level.

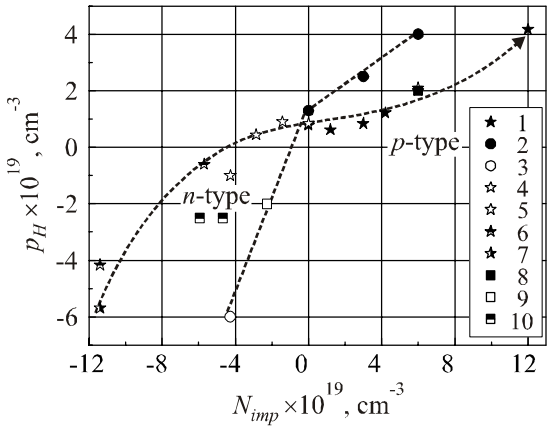

Fig. 1. The dependence of holes concentration (p_H) on impurity concentration (N imp) of Bi_2Te_3 (1 – 7) and $Bi_2Te_{3-y}Se_y$ (8 – 10): only Sn (1, 8); without Sn, only acceptor Bi, Pb (2) or donor I (3, 9) impurity; and codoped with Sn and acceptor (4) or donor (5 – 7, 10) impurity.

Fig. 1 displays a dependence of holes concentration p of Bi_2Te_3 on the amount of the introduced *Sn* impurity (N_{imp}). Also shown is the data on the codoping of Bi_2Te_3 with *Sn* and the additional *Cl*, *Pb* and *J* impurities. We observe holes concentration to vary only weakly: from $2\cdot10^{18}$ to $5\cdot10^{18}$ cm^{-3} with the tin content in $N_{imp} = (1.2 \div 6)\cdot10^{19}$cm^{-3}. So, we can speak of "soft" stabilization of the chemical potential. All single crystals of *n*- and *p*-type, doped with *Sn*, demonstrate an increase of electrical homogeneity as compared to the undoped Bi_2Te_3.

2.2. Micro-thermoprobe mapping and sample homogeneity

The spatial distribution of thermoelectric power over the surface of single crystals was investigated by a microprobe.

While the undoped crystals exhibit the usual statistical fluctuations of the Seebeck coefficient, the statistical fluctuations become smaller on the sample with 1 at.% *Sn* incorporated in the material. The respective number of measuring points of given Seebeck value contained in the mappings is represented in Fig. 2. These distributions become more focused with incorporation of *Sn*.

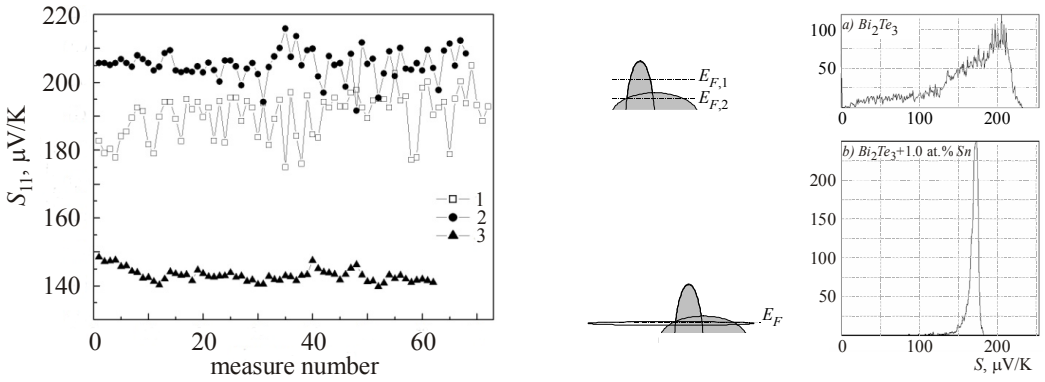

Fig. 2. On the left – the Seebeck coefficient S_{11} measured over the samples surface: 1 – $Bi_{1.9}Sb_{0.1}Te_3$, 2 – $(Bi_{1.9}Sb_{0.1})_{0.998}Sn_{0.002}Te_3$ u 3 – $(Bi_{1.9}Sb_{0.1})_{0.99}Sn_{0.01}Te_3$; on the right – statistical fluctuations of the Seebeck coefficient over the samples surface: above – Bi_2Te_3, below – Bi_2Te_3:Sn.

2.3. The temperature dependences *R*(*T*) and *S(T)* of *p*-type.

The resonance states in the valence band of Bi_2Te_3 are leading to a drastic change in the temperature dependences of the transport coefficients σ_{11}, R_{321}, S_{11} in these crystals, similarly to the way it was reported for Bi_2Te_3. The temperature dependences $R(T)$ of the samples containing *Sn* change from a rising pattern with a maximum typical for Bi_2Te_3 and $Bi_2Te_{3-x}Se_x$ to a strongly decreasing curve (Fig. 3).The Seebeck coefficient of tin-containing samples is somewhat larger in the temperature region at T = 200 K and at T = 380 K, and their dependence becomes more gently sloping with temperature (Fig. 4).

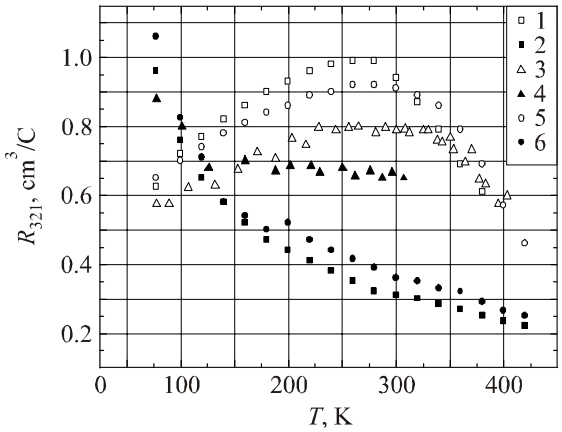

Fig. 3. R_{321} = f(T) for p-type Bi_2Te_3 (1), doped with Sn (2), under substitution Sb → Bi (3,4) and under substitution Se → Te (5, 6); open symbol – without Sn, full symbol – doped with Sn.

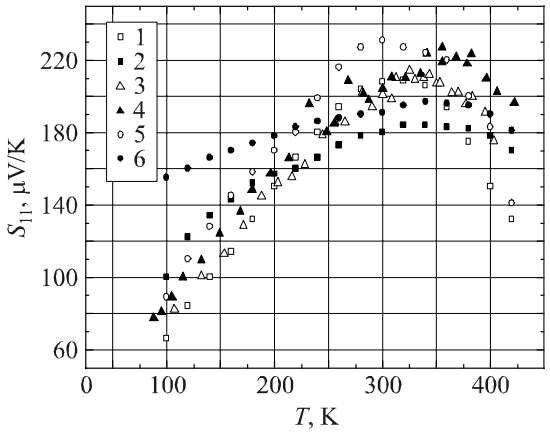

Fig. 4. S_{ij} = f(T) for p-type Bi_2Te_3 (1), doped with Sn (2), under substitution Sb → Bi (3, 4) and under substitution Se → Te (5, 6); open symbol – without Sn, full symbol – doped with Sn.

2.4. The electrical conductivity σ (hole mobility) and the Nernst-Ettingshausen coefficient Q_e/k_0

We observed a considerable drop of the electrical conductivity σ (hole mobility) and the Nernst mobility.

2.5. *n*-type. $Bi_2Te_{3-x}Se_x$ (x = 0.06; 0.12)

The doping with tin does not change the character of the temperature dependences of the transport coefficients σ_{11}, R_{321}, S_{11} in *n*-type crystals, except for a strong decrease of the Nernst mobility and its anisotropy.

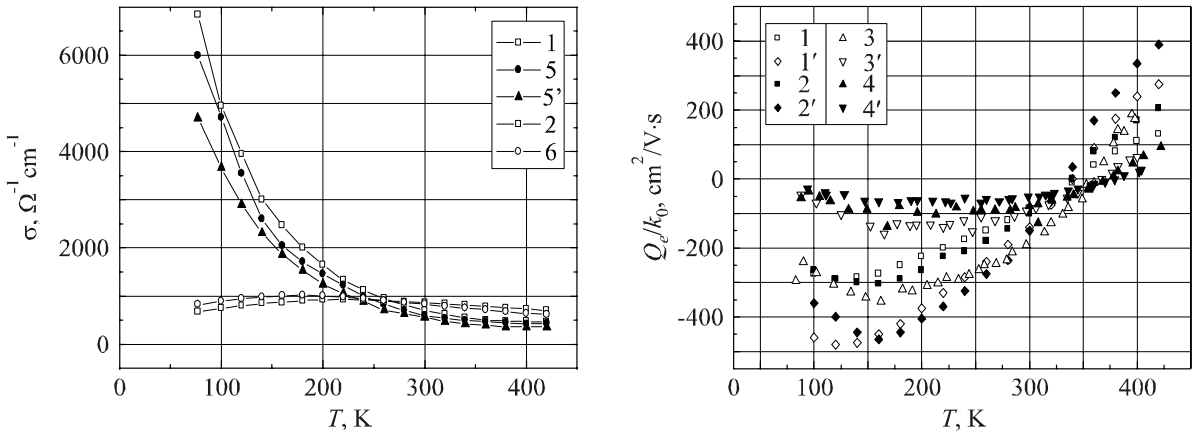

a) *b)*

Fig. 5. $\sigma_{11} = f(T)$ *(a),* $Q_e/k_0 = f(T)$ *(b) for p-type* Bi_2Te_3 *(1), doped with Sn (2), under substitution Sb → Bi (3, 4) and under substitution Se → Te (5, 6); open symbol – without Sn, full symbol – doped with Sn.*

3. Discussion and computer simulation

To solve the problem of the influence of resonant states on the concentration of carriers (holes) related to a group of crystal defects in $A^{V}B^{VI}$ compounds, we employed the same method as for *PbTe*-based solid solution [7].

The chemical potential of holes μ, measured from the top of the valence band, can be found from the condition for the thermodynamic potential minimum:

$$\Phi = H_v n_v - kTn_v\left(\ln N / n_v + 1\right) + \Phi_e, \tag{1}$$

where n_v is the vacancy concentration, N is concentration of the sites in the metal sublattice, and H_v is the enthalpy of formation of one vacancy involving the transfer of two electrons from the bottom of the conduction band to this vacancy.

The thermodynamic potential of electrons Φ_e differentiated with respect to the total electron density n_e (i.e., at the density of electrons in the conduction band, in the valence band and at impurity centers) gives the chemical potential μ. Since each metal vacancy absorbs two electrons, it follows that

$$\partial n_e / \partial n_v = 2, \text{ which gives } \partial\Phi_e / \partial n_v = 2\mu. \tag{2}$$

Differentiating Eq. (1) with respect to n_v and equating the derivate to zero, we obtain the equation for μ, the solution of which can be represented in the form

$$\mu^* = H_v^* / 2 + 1/2 \cdot \ln\left(n_v / N\right). \tag{3}$$

We supposed, as mentioned in [8], that one can estimate the concentration of free carriers (holes) as $[h^{\cdot}] = [Bi'_{Te}] - 2[V^{\cdot\cdot}_{Te}]$. The concentration of free charge carriers in the undoped bismuth telluride can be expressed by means of the following relation:

$$\left[h^{\cdot}\right] = N_{AS} - N_V = k_1\left[Bi_{Bi}\right]/2\exp\left(-E_{AS}/k_BT_m\right) - 2\left[Te_{Te}\right]\exp\left(-E_V/k_BT_m\right), \tag{4}$$

where $k_1 \sim 1.2$ is a statistical parameter referring to the description of the formation of one antisite defect in Bi_2Te_3. E_{AS} and E_V stand for the energy of formation of antisite defects. $V^{\cdot\cdot}_{Te}$ – vacancies in the tellurium sublattice, k_B is the Boltzman constant, T_m is the melting point, $[Bi_{Bi}]$ is the number of *Bi* atoms per 1 m^3, $[Te_{Te}]$ is the number of *Te* atoms per 1 m^3, N_{AS} is the concentration of antisite defects, N_V is the concentration of vacancies of *Te*.

The electrical neutrality equation is

$$N_{Sn} - n_{Sn} + \left[Bi'_{Te}\right] - 2\left[V^{\cdot\cdot}{}_{Te}\right] = p + n, \tag{5}$$

where N_{Sn} is the concentration of the *Sn* impurity atoms, n_{Sn} is the density of electrons at the impurity levels, p and n are the densities of holes and electrons, respectively. If it is supposed that the impurity band has two states per atom, this will imply that

$$n_{Sn} = 2N_{Sn} / [1 + \exp(\varepsilon^*_i - \mu^*)],$$

where ε^*_i is the position of an impurity level relative to the top of the valence band. If the densities of free carriers are expressed in terms of the Fermi integrals $F_{1/2}$, we find

$$N_c F_{1/2}\left(\mu^*\right) - N_v F_{1/2}\left(\mu^* - \varepsilon_g\right) = N'_{Sn} + \left[N_{imp}\right], \tag{6}$$

where N_c, N_v are the effective densities of states in the conduction and valence bands;

$$N'_{Sn} = N_{Sn}\left[1 - \exp\left(\varepsilon^*_i - \mu^*\right)\right] / \left[1 + \exp\left(\varepsilon^*_i - \mu^*\right)\right],$$

ε_g is the energy gap between the conduction and valence band,

$$N_{imp} = N''_{Sn} + E_{AS} - E_V,$$

N''_{Sn} is part of *Sn* atoms placed in Te^{II} positions, where they give holes and do not create the resonance levels.

We solved numerically the equation for the equilibrium concentration of vacancies and antisite defects at the melt temperature T_m by minimization of the thermodynamic potential. Then, assuming that the number of vacancies and antisite defects is independent of temperature, we solved the electrical neutrality equation (6) for (n-p) at the measurement temperature.

The electrical neutrality equation (6) was solved numerically with the following assumptions:

$e_i = 0.015$ eV; $N_{Sn} = [0, 2.4]\cdot 10^{19}$; $e_{g0} = 0.2$ eV; $\alpha = -1.5\cdot 10^{-5}$; $k = 0.86\cdot 10^{-4}$.

The impurity level is situated in the valence band:

$e_g^* = (e_{g0} + \alpha\cdot T)/(k_0\cdot T)$; $e_c = 0.02$ eV; $m_{dn1}{}^* = 0.35$; $m_{dn2}{}^* = 1$; $m_{dn} = 0.8$; $m_{dp} = 0.66$.

Results of the computer calculations of (n-p) versus N_{imp} are presented in Fig. 8.

We can see the action of resonant level ε^*_i on the hole and electron concentration that is related to the position of an impurity level relative to the top of the valence band and the Fermi level.

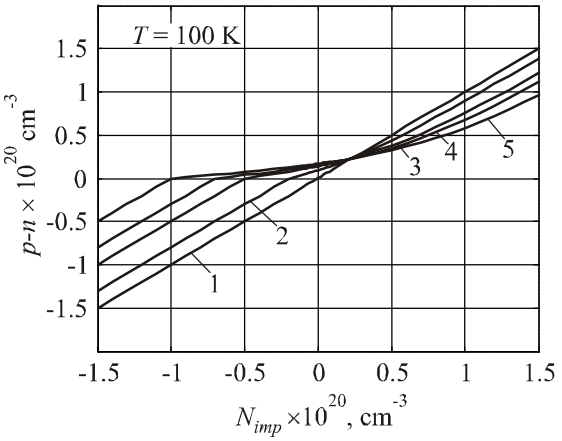

Fig. 7. The dependences of the difference p-n = f(N_{imp}) on impurity concentration (N_{imp}) at different values N_{Sn} (1 – 5): (0, 1.2, 3, 4.2, 6)·10^{19} cm^{-3}.

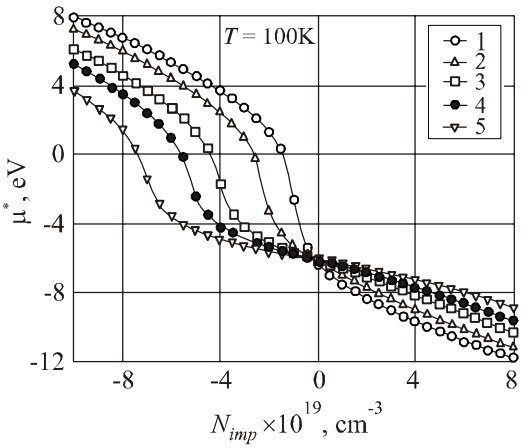

Fig. 8. The dependences of the Fermi level (μ^*) on impurity concentration (N_{imp}: N_A, N_D). Curve numbers at different values N_{Sn} (1 – 5): (0, 1.2, 3, 4.2, 6)·10^{19}cm^{-3}. Position of Sn impurity level ε_i = 0.02 eV relative to the top of the valence band.

We can observe different action of resonant level ε^*_i on the Fermi level for *p*- and *n*-type, when it is situated in the valence band. The dependence of the Fermi level on the acceptor concentration N_A has a gentle initial dip with increasing the number of *Sn* atoms. By this is meant that the Fermi level is less dependent on N_A introduced in the samples. The Fermi level dependence on the donor concentration N_D is of the same character as at doping with ordinary acceptor impurity.

We can see from Fig. 9 *a* that dependences of *S* on the impurity concentration change at doping with *Sn* atoms. They become more gently sloping for *n*- and *p*-type samples in the range of concentration generally used in thermoelectric devices, just at $N_{imp} = (0.8 \div 3)\cdot 10^{19}$ cm^{-3}.

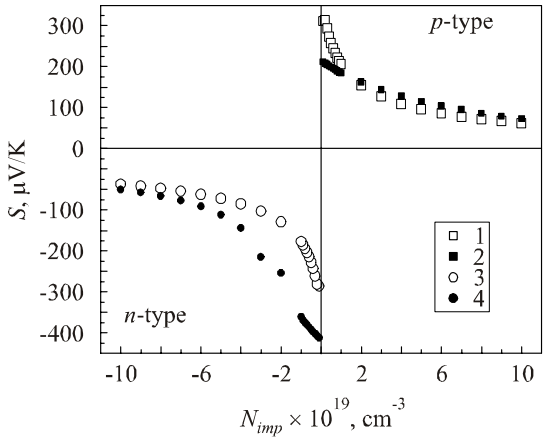

Fig. 9 a. The numerical calculations of $S = f(N_{imp})$ are shown in different scales (+ $N_{imp} = N_{acc}$; – $N_{imp} = N_d$): 1, 2 – p-type; 3, 4 – n-type. 1, 3 – without Sn; 2, 4 – N_{sn} = 2, 4·10^{19} cm^{-3}.

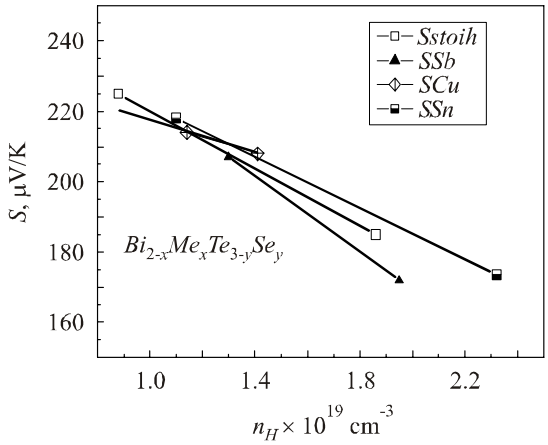

Fig. 9 b. The experimental dependence of the Seebeck coefficient S on the electron concentration n.

We used both our own experimental data and the results of computer simulation for numerical estimation of the electron density concentration on the distribution of the *n*-type Seebeck coefficient. We employed the formula from [9]:

$$\Lambda_{eff} = \Lambda\left(\langle n\rangle\right)\left[1 + g\frac{\left\langle\left(\delta n\right)^2\right\rangle}{\langle n\rangle^2}\right],$$

where $\Lambda = S$, g is power exponent in the dependence of S on the concentration of electrons (holes): $S \sim n^g$. $g = 0.4$ for samples without *Sn*, and $g = 0.25$ for samples doped with *Sn*. Parameter g for different solid solutions was found from the experiments and by calculation. We obtained the following values for *p*-type: $\Delta N/N \approx 15\%$, $\Delta S/S \approx 5\%$ for samples without *Sn* and $\Delta N/N \approx 6\%$ and $\Delta S/S \approx 2\%$.

The results of computer calculations of S_{11} and R_{321} versus temperature are presented in Fig. 10, 11.

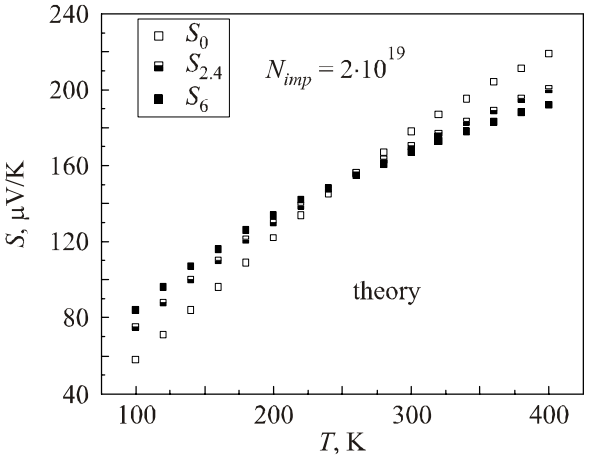

Fig. 10. Temperature dependences of the Seebeck coefficient S_{11} for Sn-doped samples are more gently sloping than for the undoped samples.

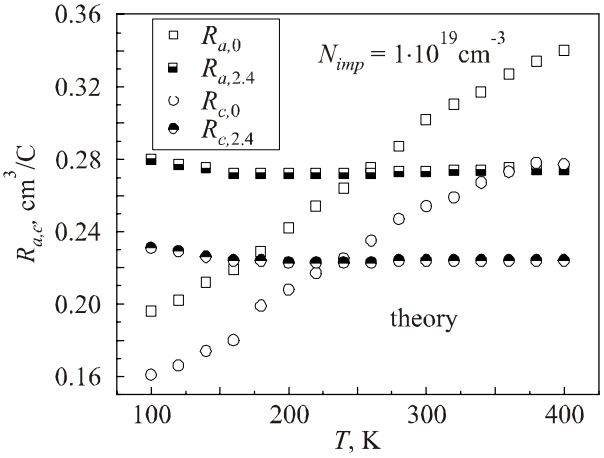

Fig. 11. Temperature dependences of the Hall coefficient R_{321} change from "conventional", for the undoped solid solution, to strongly decreasing as the temperature rises, for Sn-doped samples.

Computer simulation of the Seebeck and Hall coefficients for *p*-type solid solution shows changes in the temperature dependences. They prove strong influence of the resonant states on the *S(T)* and *R(T)* for *p*-type.

So, our calculations support the concept of the influence of *Sn* states, placed on the background of the allowed valence band spectrum for *p*-type solid solution. But homogeneity increase of *n*-type crystals doped with *Sn* has another explanation. The *X*-ray photoelectron spectroscopy [10] was used to show that *Sn* atoms incorporated into the lattice $Bi_2Te_{2.85}Se_{0.15}$ interact with *Bi* and *Te* atoms. They redistribute the densities of electron states in the valence band, change the binding energies and chemical shifts of the core levels. This feature of the energy spectrum affects the volume distribution of the doping defects. Their number is reduced, leading to a high electrical homogeneity.

Conclusion

The results obtained in this work on the influence of *Sn* impurity on the electrical homogeneity of Bi_2Te_3 and $Bi_2Te_{3-y}Se_y$ single crystals argue for essential influence of *Sn* impurity states placed within the valence band on the thermoelectric properties of *p*- and *n*-type crystals.

The *Sn* atoms incorporated into $Bi_2Te_{2.85}Se_{0.15}$ lattice redistribute the density of electron states in the valence band, change the binding energies and chemical shifts of the core levels. This feature of the energy spectrum affects the volume distribution of the doping defects. Their number is reduced, leading to a high electrical homogeneity of both *p*- and *n*-type.

The thermoelectric parameters of *n*-type crystals have been improved and reach the value of

$$Z = 3.3 \cdot 10^{-3}\,\mathrm{K}^{-1}.$$

The computer program written and the numerical results obtained in this work enable a quantitative estimation of the effect of different impurity atoms on the hole and electron concentration. The calculations confirm the validity of the physical model chosen for consideration in this work. The numerical results are in good agreement with the experimental data.

References

1. V.A. Kulbachinskii, M. Inoue, M. Sasaki, H. Negishi, W.X. Gao, K. Takase, Y. Giman, J. Horak and P. Lostak, *Phys. Rev. B* **50,** 16921 (1994).
2. M.K. Zhitinskaya, S.A. Nemovand T.E. Svechnikova, *Physics of the Solid State* **40**, 1428 (1998).
3. M.K. Zhitinskaya, S.A. Nemov, T.E. Svechnikova, P. Reinshaus and E. Muller, *Semiconductors* **34,** 1363 (2000).
4. I.V. Gasenkova, A. Chubarenko, E.A. Tyavlovskaya and T.E. Svechnikova, *Semiconductors* **37**(6), 661(2003).
5. T.E. Svechnikova, S.N. Chizhevskaya and N.M. Maksimova, *Inorganic Mater*. **30,** 161 (1994)
6. D. Platzek, G. Karpinski, C. Drasar, E. Miller Seebeck Scanning Microprobe for Thermoelectric FGM Conf. on Thermoelectrics (ICT2003), La GrandeMotte, France, IEEE, Piscataway 2004, p. 528 – 531.
7. S.A. Nemov, Yu.I. Ravich, M.K. Zhitinskaya and V.I. Proshin, *Sov.Phys.Semicond*. **26**(8), 839 (1992).
8. S. Karamazov, P. Lostak, J. Horak and R. Kuzel, *Phys.Stat.Sol.(a)* **148**, 229(1995).
9. M.K. Zhitinskaya, *Izv.Vuz. Fizika* 4, 1985 (in Russian).
10. I.V. Gasenkova, M.K. Zhitinskaya, S.A. Nemov and T.E. Svechnikova, *Physics of the Solid State* **41** (11), 1805 (1999).

Submitted 10.05.2011.